MOLECULAR AND CELLULAR BIOLOGY, July 2008, p. 4331–4341 Vol. 28, No. 13
0270-7306/08/$08.00+0 doi:10.1128/MCB.00519-07

Involvement of Importin-4 in the Transport of Transition Protein 2 into the Spermatid Nucleus▽

M. M. Pradeepa,[1] S. Manjunatha,[1] V. Sathish,[1] Shipra Agrawal,[1]† and M. R. S. Rao[1,2]*

Jawaharlal Nehru Centre for Advanced Scientific Research, Jakkur, Bangalore 560064,[1] and Department of Biochemistry, Indian Institute of Science, Bangalore 560012,[2] India

Received 26 March 2007/Returned for modification 11 May 2007/Accepted 26 July 2007

Mammalian spermiogenesis is characterized by a unique chromatin-remodeling process in which histones are replaced by transition protein 1 (TP1), TP2, and TP4, which are further replaced by protamines. We showed previously that the import of TP2 into the haploid spermatid nucleus requires the components of cytosol and ATP. We have now carried out a detailed analysis to characterize the molecular components underlying the nuclear translocation of TP2. Real-time PCR analysis of the expression of different importins in testicular germ cells revealed that importin-4 and importin-β3 are significantly up-regulated in tetraploid and haploid germ cells. We carried out physical interaction studies as well as an in vitro nuclear transport assay using recombinant TP2 and the nuclear localization signal of TP2 ($TP2_{NLS}$) fused to glutathione *S*-transferase in digitonin-permeabilized, haploid, round spermatids and identified importin-4 to be involved in the import of TP2. A three-dimensional model of the importin-4 protein was generated using the crystal structure of importin-β1 as the template. Molecular docking simulations of $TP2_{NLS}$ with the importin-4 structure led to the identification of a $TP2_{NLS}$ binding pocket spanning the three helices (helices 21 to 23) of importin-4, which was experimentally confirmed by in vitro interaction and import studies with different deletion mutants of importin-4. In contrast to TP2, TP1 import was accomplished through a passive diffusion process.

A hallmark of eukaryotic cells is the presence of different subcellular compartments that are surrounded by membranes that are impermeable to macromolecules. Specific transport systems have evolved to allow nuclear proteins to be imported from the cytoplasm. While proteins of less than 45 kDa passively diffuse through the nuclear pore complex, proteins larger than 45 kDa are transported through an active process involving the specific recognition of nuclear localization signals (NLSs) by suitable receptors present in the cytoplasm (26). The best-characterized transport process that is involved in the majority of nuclear proteins is characterized by the recognition of NLS sequences by importin-α present in the importin-α/β heterodimer (13, 17, 41) along with Ran and its binding protein, nuclear transport factor (1, 39). Importin-α provides the NLS binding site (2), which contains the *armadillo* motifs and interacts with importin-β with its N-terminal importin-β binding domain. The transport of the trimeric complex (cargo/importin-α/β) into the nucleus is facilitated by the interaction of importin-β with nuclear pore complex proteins (18). Inside the nucleus, Ran in its GTP-bound form binds to importin-β, dissociating the complex and thereby releasing importin-α and its cargo (16).

Although many of the proteins are imported by an importin-α/β-dependent pathway, some proteins are imported into the nucleus by importin-β (40, 49) or importin-α alone (27). In addition, many variants within the α and β proteins that are involved in the import of specific nuclear proteins have been discovered. Recently, a new group of importins related to β-importins (also called orphan importins) that can interact with the NLS of a specific cargo and transport it into the nucleus independently of importin-α has been described. For example, importin-4 is involved in the nuclear import of ribosomal protein S3a (rpS3a) (25) as well as vitamin D receptor (VDR) (38). Importin-9 (25) and importin-11 (42) are involved in the transport of ribosomal proteins S7 and L12, respectively. Importin-7 is involved in the transport of human immunodeficiency virus type 1 (HIV-1) intracellular reverse transcription complexes (11), while importin-13 mediates the nuclear accumulation of the SUMO-conjugating enzyme human UBC9 (37). Importin-β3 is involved in the nuclear import of ribosomal protein (24). The importin family of proteins, in addition to taking part in the nuclear import pathway, is implicated in having a secondary role particularly with respect to highly basic proteins like histones and ribosomal proteins. By complexing with basic proteins, they shield them against any undesired interactions with other cellular components and also prevent them from aggregating (25).

Mammalian spermatogenesis is a unique cellular differentiation system in which there is a continuous and dramatic change in nuclear morphology and chromatin structure. The most dramatic changes occur in haploid germ cells following meiotic division in the spermiogenesis process. This process is divided into 19 stages, and during stages 12 to 15, nearly 90% of the histones (including both somatic and testis-specific histones) are replaced by transition protein 1 (TP1), TP2, and TP4, which are subsequently themselves replaced by protamines. Both TP1 (6.5 kDa) and TP2 (13 kDa) are highly basic

* Corresponding author. Mailing address: Jawaharlal Nehru Centre for Advanced Scientific Research, Jakkur, Bangalore 560064, India. Phone: 91-80-2208 2864. Fax: 91-80-2362 2762. E-mail: mrsrao@jncasr.ac.in.

† Present address: Institute of Bioinformatics and Applied Biotechnology, ITPL, Bangalore 560066, India.

▽ Published ahead of print on 6 August 2007.

proteins that have unique biochemical properties, and $TP1^{-/-}$ and $TP2^{-/-}$ mice are infertile (53). During the transition phase, round spermatids must import these basic proteins into the nucleus. We recently showed that the import of TP2 into the haploid spermatid nucleus is an active process and hence involves one of the import mechanisms (51). Here, we describe a detailed study on the components involved in this import process and show that importin-4 is involved in transporting TP2 and interacts with the NLS sequence of TP2. In contrast to TP2, TP1 is transported into the haploid nucleus by passive diffusion. We have also modeled the three-dimensional (3D) structure of importin-4. The docking of this structure with the NLS of TP2 ($TP2_{NLS}$) revealed that the three helices (helices 21 to 23) of the importin-4 protein contribute to the $TP2_{NLS}$ binding pocket, which was experimentally confirmed with various deletion mutants of importin-4.

MATERIALS AND METHODS

Oligonucleotides were synthesized and procured from Sigma. Importin-4 polyclonal antibodies were raised by immunizing a female New Zealand White rabbit with recombinant importin-4. TP2 and TP1 antibodies were raised in a male New Zealand White rabbit using recombinant and in vivo proteins, respectively. Anti-glutathione *S*-transferase (anti-GST) (polyclonal) and anti-His-tagged (monoclonal) antibodies were obtained from Sigma. Goat anti-rabbit secondary antibodies conjugated with Alexa Fluor 488 dye were purchased from Molecular Probes. Adult male Wistar rats (*Rattus norvegicus*; 55 days old) were used for the purification of different spermatogenic cells by centrifugal elutriation (46). All procedures for handling animals were approved by the animal ethics committee of the Jawaharlal Nehru Centre for Advanced Scientific Research. Isolated cells were analyzed by fluorescence-activated cell sorter (FACS) analysis to check for the purity of cells, and the cytosol was prepared from round spermatids (51).

Cloning, protein expression, and purification. The NLS of TP2 (^{87}GKVSKR KAV^{95}) was cloned at the C terminus of GST in vector pGEX-2T, expressed in BL21(DE3) cells, and purified using a glutathione-agarose column (Sigma). The nucleotide sequence coding for TP2-NLS was verified by DNA sequencing and Western blot analysis with anti-TP2 polyclonal antibodies, which recognize TP2-NLS in the GST-$TP2_{NLS}$ fusion protein. Rat TP2 cloned in vector pET22b and expressed in BL21(DE3) cells was purified by heparin-agarose column chromatography (36). His-tagged human importin-4 protein was purified from vector pQE80 (a gift from D. Gorlich) with a nickel-nitrilotriacetic acid (NTA) column (Qiagen) (25). A deletion mutant of importin-4 (deletion of residues 529 to 609 [Δ529–609]) lacking the $TP2_{NLS}$-interacting domain was generated by sequential three-piece ligation. N-terminal importin-4 (fragment A) was released from wild-type importin-4 in vector pQE80 by EcoRI digestion. The C-terminal fragment of importin-4 (fragment B) was generated by PCR amplification from the vector DNA with inclusion of an EcoRI site in the forward primer and a HindIII site in the reverse primer. The PCR product was digested with the above enzymes, and fragment A and fragment B were allowed to ligate, followed by addition of vector DNA digested with EcoRI and HindIII. To generate a C-terminal deletion construct lacking the C-terminal domain, wild-type importin-4 in vector pQE80 was digested with SacI, which releases C-terminal importin-4 (amino acid residues 607 to 1081), and the N-terminal importin-4 in vector pQE80 was religated. The mutant importin-4 was expressed and purified as described above for the wild-type importin-4. The complete coding region of rat importin α6 (NM_001015029) was amplified from cDNA synthesized from round spermatid cells and was cloned into the SphI/BamHI sites of vector pQE70. Protein was expressed in BL21 cells and purified with a Ni-NTA column. GST-tagged mouse importin-α1 and mouse importin-β1 were purified from vector pGEX2T (a gift from Y. Yoneda) with a glutathione-agarose column (Sigma) (21). Human importin-α3 (in vector pQE60) was a kind gift from M. Kohler, and the protein was expressed and purified with a Ni-NTA column (14). Human importin-β2 in vector pQE60 (a gift from D. Gorlich) was expressed and purified with a Ni-NTA column (22). *Xenopus* importin-7 in pQE9, a gift from D. Gorlich, was expressed and purified as described previously (24). Mouse importin-9 in pQE80 was expressed and purified as described previously (25). Ran and RanQ69L (a GTPase mutant of Ran which is loaded with GTP) in pQE32 (gifts from D. Gorlich) were purified by Ni-NTA-agarose as described previously (16). Human VDR was PCR amplified from pEBFPC-1 vector (a gift from Noa Noy). After digestion with BamHI/EcoRI, the DNA fragment was subcloned into pGEX 4T1 and the expressed protein was purified with a glutathione-agarose column (Sigma). Polypyrimidine tract binding protein (PTB) in pET22b was expressed in BL21 cells and purified by ammonium sulfate precipitation followed by heparin-agarose and poly(U) agarose column chromatography (15). The sequence for rat importin-α4 (NM_001014793.1) was cloned into the BamHI and XhoI sites of pGEX4T1; the sequence for rat importin-13 (BC100658) encoding amino acids 332 to 963, which is known to bind to its cargo glucocorticoid receptor (48), was cloned into the BamHI and EcoRI sites of pGEX4T1; and the expressed GST fusion protein was purified with a glutathione-agarose column. Mouse importin-β3 (BC054814), which has a 98% identity to predicted rat importin-β3 (XM_224534), was amplified from a cDNA clone purchased from Open Bio Systems and ligated to the SmaI and XhoI sites of pGEX4T1, and the expressed GST fusion protein was purified with a glutathione-agarose column. All the clones were verified by DNA sequencing using appropriate primers with an ABI Prism 3100 sequencer.

Real-time PCR analysis. RNA was isolated from gametic diploid, haploid, and tetraploid cells using TRIzol reagent (Invitrogen). Testis from 10-day-old rats served as a source of gametic diploid cells. After treating total RNA with DNase I (Sigma), reverse transcription was carried out with 2 μg of RNA using avian myeloblastosis virus reverse transcriptase (NEB). Random hexamer primers were used for first-strand cDNA synthesis. To design primers for real-time PCR, most of the mRNA sequences coding for rat importins were downloaded from the NCBI database, except that importin-8 was initially amplified using mouse importin-8 primers and after the amplicon was sequenced, internal rat-specific primers were designed for real-time PCR. Primers were designed for each of the importins using primer 3 software to amplify the 300- to 400-bp region of each of the importins. Specificity of these primer pairs was monitored by agarose gel electrophoresis of the PCR product, and amplicons were further verified by DNA sequencing. Melt curve analysis was also performed to ensure specific amplification without any secondary nonspecific amplicons. PCR products were prepared in a final volume of 20 μl using iQ Sybr green supermix (Bio-Rad). We also performed a control PCR without carrying out the RT step to make sure that we were not amplifying pseudogenes in the contaminating genomic DNA. Real-time PCR analysis was repeated five times with an i-Cycler iQ (Bio-Rad) using the following reaction conditions: 95°C for 5 min (initial denaturation); 95°C for 15 s, 55 to 56°C for 1 min, and 72°C for 30 s for 40 cycles; and final extension at 72°C for 5 min. Difference in C_T (threshold values) were used to calculate the difference in expression of mRNA in gametic diploid (2n), tetraploid (4n), and haploid (n) cells by the $\Delta\Delta C_T$ method ($2^{-\Delta\Delta C_T}$) of analysis. Standard deviation of the mean was calculated by standard methods. Nascent polypeptide-associated complex alfa (NACA) was used as an internal normalization control, as its expression level across different stages of germ cell differentiation was found to be unaltered in our microarray experiments. The details of the primer pairs used for PCR amplification of different importins are given in Table 1.

In vitro import assay. Nuclear import of exogenously added cargoes (recombinant TP2, GST-NLS_{TP2}, PTB, VDR, and TP1) was studied in vitro using digitonin-permeabilized round spermatids as described previously (51). Briefly, round spermatids obtained after centrifugal elutriation were washed with ice-cold transport buffer {20 mM HEPES, pH 7.3, 100 mM potassium acetate, 5 mM sodium acetate, 2 mM dithiothreitol, 1 mM EGTA, and protease inhibitor mixture [4-(2-aminoethyl) benzenesulfonyl fluoride, pepstatin A, E-64, bestatin, leupeptin, and aprotinin; 1 μg/ml; Sigma]}. Cells were then permeabilized in transport buffer containing 40 μg/ml digitonin (Sigma) at 0°C for 5 min and subsequently washed with cold transport buffer. In vitro transport was initiated in 50 μl transport buffer containing round spermatid cytosol (51) or recombinant importins, TP2, and 1 mg/ml bovine serum albumin with an energy regeneration system (0.5 mM ATP, 0.5 mM GTP, 5 mM creatine phosphate, and 20 units/ml creatine phosphokinase). In the indicated experiments, the import reaction was carried out in the absence of an energy-regenerating system and in the presence of GTPase mutant Ran (RanQ69L) or by preincubation of digitonin-permeabilized cells with wheat germ agglutinin (WGA) (Sigma) for 10 min at 4°C. To deplete importin-4, round spermatid cytosol was incubated with anti-importin-4 antibodies for 1.5 h at 4°C. Protein A-agarose (Invitrogen) was added to the cytosol for an additional 2 h at 4°C and removed by centrifugation. Depletion of importin-4 from the cytosol was ascertained by Western blot analysis with importin-4 antibodies. PTB and GST-VDR were used as controls in import assays along with TP2. For reconstitution experiments, purified recombinant importin-4 (0.1 mg/ml) was added to the immunodepleted cytosol. The import reaction was carried out at 30°C for 30 min. After fixing the cells with 4% paraformaldehyde, immunofluorescence was performed using anti-TP2/anti-TP1/anti-GST/anti-PTB antibodies and secondary anti-rabbit antibodies conjugated with Alexa Fluor 488.

TABLE 1. Primer pairs used for real-time PCR of different importins

Serial no.	Protein	Primer(s) (5′–3′)		GenBank accession no.	Amplicon size (bp)	Representative cargo(s) (reference)
		Forward	Reverse			
1	Importin-α1	ATTGCAAACAGCAGAGTTCC	GTCCTCCGTCCCAAAGTAAT	NM_198726	361	Sgk (32), PTB (45), STAT1 (35)
2	Importin-α2	CTCCTACACCACAACGATCC	CTGCCTTAGAGAGGACACCA	NM_053483	394	NBS1 (50)
3	Importin-α3	AGTTCAGGAGATTTTGCCAGC	TCGATCACAGCCTGAACTTG	NM_001014792.1	347	STAT3 (30), RNA helicase A (4)
4	Importin-α4	CAGCAGGTTCAGGCAGTAAT	ATTTTCTCCAGTCCACCACA	NM_001014793.1	310	NF-κB (10)
5	Importin-α6	TGAAGAAGCTGCCATGTTTG	GGTCTGCTGAGAGGTTCCAG	NM_001015029	309	None
6	Importin-β1	ACGTTCCTGGTGGAACTGTC	ATGGCTTCCAGTGTGGACTC	NM_017063.1	355	HIV Tat (49), HIV Rev (19), SREBP-2 (29), cyclin B1-Cdc2 (47)
7	Importin-β2	GTTCGGCAGAGTTCTTTTGC	CATTCCGTGGGATTTGTACC	BC090323	335	Ribosomal proteins (24), mRNA binding proteins (44)
8	Importin-β3	TCAGGAACATCCTTCGATCC	GACAGCGTCACGATCACTTC	XM_224534	312	Ribosomal proteins (24)
9	Importin-4	GCTGCCTCACTTTCTTGGTC	TGCAGCAGTGGGTATAGCAG	NM_001106038	384	rpS3a (25), VDR (38)
10	Importin-7	CTTGGCCTGTGTGCTCTTAT	CAGGGTTATCCTCATCATCG	NM_001107545.1	352	H1 (23), HIV-1 intracellular reverse transcription complexes (11)
11	Importin-8	GAGCTGGCTTGGCAGTTTAC,[a] GCAAATCCTGCAGCTGC TTC[b]	ACCTGTTGAAATCCCACTGCC,[a] CATACCGTTCAAAGAGACG[b]	NM_001081113.1	480,[a] 339[b]	SRP19 (9)
12	Importin-9	ATGCATGGGTTCCTGACTAA	CTGGGCTGCTAGGTGAATTA	NM_001107180	303	rpS7 (25)
13	Importin-11	GTCGGTGAAGGCGTTACATT	AGTGCAAGGCCTCAAACTGT	XM_001064746	308	UbcM2 (42), rPL12 (43)
14	Importin-13	ACTCGACAGTTGGTCCACAT	GAGGCAGCAGCTCAGTAAAG	BC100658	301	UBC9 (37), glucocorticoids (48)
15	NACA	ATGTCCAAACTGGGTCTTC	GGACAGCCTTTGCTCTTGAC	XM_213821	332	NA

[a] Mouse primer.
[b] Rat primer.

Images were captured with a confocal laser scanning microscope (LSM 510 META; Carl Zeiss).

Immuno-pull-down assay. Ten microliters of protein A-agarose (Invitrogen) was incubated with 20 μg of either preimmune serum or TP2 monospecific antibodies in phosphate-buffered saline (137 mM NaCl, 2.7 mM KCl, 10 mM Na_2HPO_4, 2 mM KH_2PO_4, pH 7.4) for 1 h, followed by washing once with phosphate-buffered saline. The antibody-bound beads were incubated with bacterially expressed TP2 along with importin-α1, importin-α3, importin-α4, importin-α6, importin-β1, importin-β2, importin-β3, importin-4, importin-7 and importin-9, C-terminal importin-13 (amino acids 332 to 936), Δ529-609 importin-4, or ΔC-terminal importin-4 in binding buffer A, containing 20 mM HEPES (pH 7.3), 100 mM Nacl, 10% glycerol, 2 mM dithiothreitol, 5 mM $MgCl_2$, and 0.1 mM phenylmethylsulfonyl fluoride for 3 h, followed by three washes with the same buffer. The bound proteins were separated by sodium dodecyl sulfate (SDS)–8% polyacrylamide gel electrophoresis (PAGE), transferred onto a nitrocellulose membrane, and probed with anti-His-tagged monoclonal antibody (Sigma) to detect histidine-tagged importins and anti-GST antibodies (Sigma) for the detection of GST-tagged importins. Similarly, the interaction of RanGTP with wild-type and mutant (Δ529-609) importin-4 was checked after the pull-down experiment by using an anti-His-tagged monoclonal antibody to detect six-histidine-tagged RanGTP.

GST pull-down assays. GST-NLS_{TP2}, GST, and VDR proteins were immobilized on glutathione-Sepharose beads (Sigma) in binding buffer A for 1 h at 4°C. Recombinant importin-4 or round spermatid cytosol, in the presence or absence of RanQ69L (GTPase mutant of Ran loaded with GTP), was added to glutathione-Sepharose 4B beads coupled with GST, GST-NLS_{TP2}, or GST-VDR and incubated at 4°C for 4 h, followed by three washes with the same buffer. Bound fractions were separated by SDS–8% PAGE, and importins were detected by Western blot analysis with antihistidine-tagged monoclonal antibody.

Structural modeling of importin-4 and docking studies. PSI BLAST searches were performed to identify the best templates for importin-4 using the BLOSUM-62 matrix. Human importin-β1 (accession no. 1ukl) was identified as the closest sequence homologue (25% similarity without gaps), which was used as the template to model human importin-4. Consensus secondary structure prediction was done at NPS@server. The mismatched and nonconserved regions in the secondary structure alignment were edited to optimize the template and target alignment up to 39.7%. The backbone was modeled using the Swiss model server, and the side chains were added from the rotamer library. Loop modeling was done using CODA software, and the energy minimization operations were performed with GROMACS. After several rounds of loop fitting and refinement, the final 3D model was evaluated for the structural quality. The model validation was done at WHAT IF and iMoltalk servers (bonded, nonbonded interaction, main chain, side-chain parameters, G factor, and Ramachandran plot analysis). The backbone and side-chain root mean square deviation between the model and template was 0.69 Å. Molecular simulation and the docking of the importin-4 structure with $TP2_{NLS}$ were performed using Hex 4.5 software. The docking calculations were done using 3D parametric functions of both the importin-4 and NLS models, which were used to encode surface shape, electrostatic charge, and potential distributions. The parametric functions are based on expansions of real orthogonal spherical polar basis functions. The docking was performed in full rotation mode; both importin and NLS were taken at the 180° range for 1,000 solutions. To validate our procedure in other known importin-cargo interactions, we performed the same modeling and docking simulations for docking hnRNP A1 NLS to importin-β2 and SREBP2 bound to importin-β1.

RESULTS

The aim of this study was to identify and characterize the components of the import machinery that are involved in the transport of the two major nuclear basic proteins, TP1 and TP2. Previous work from our laboratory showed that the import of TP2 into the spermatid nucleus is an active process, suggesting that specific receptors of the importin family of proteins might be involved in the recognition of NLS-TP2, facilitating its transport into the nucleus (51). We carried out initial experiments on expression profiling of importin family proteins in round spermatids to identify the potential importin family member(s) that TP2 utilizes for its transport.

Expression profiling of importins at different stages of spermatogenesis. Although most importins are known to be ubiquitously expressed, there are differences in the expression levels in different testicular cell types (20, 31). In the present study, we have included all known importin family genes, including the orphan receptor genes, to study their expression pattern in germ cells of different stages of differentiation. The

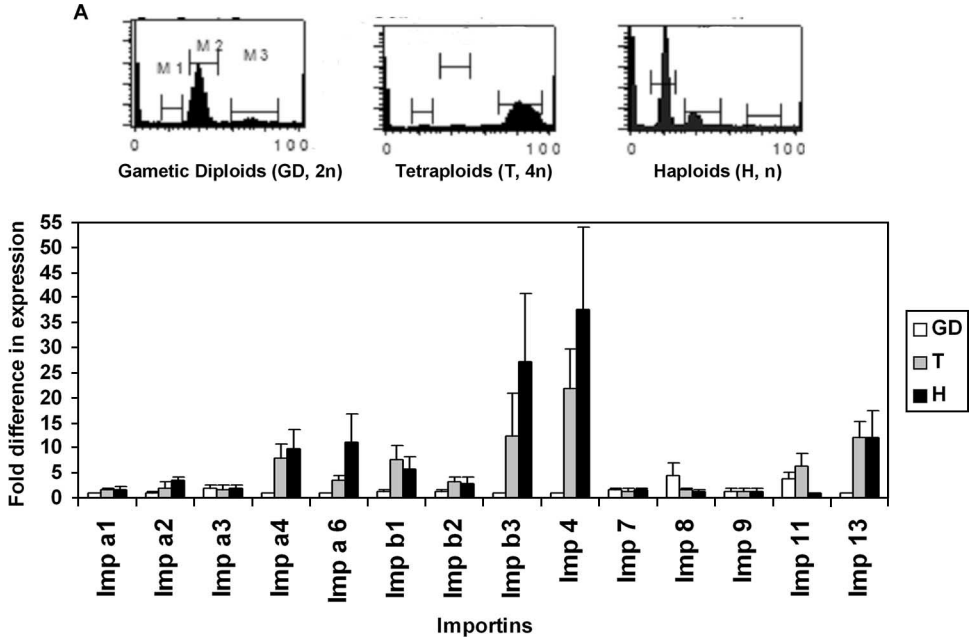

FIG. 1. Expression pattern of importins in spermatogenic cells. (A) FACS profile of diploid, tetraploid, and haploid germ cells purified from rat testes. (B) Real-time PCR analysis of importins. NACA1 was used as a normalization control. Differences in expression of importins were compared in tetraploid, haploid, and gametic diploid cells, keeping low-expressing cells as the reference. Each value plotted represent an average from five independent experiments ± standard deviation. GD, gametic diploid germ cells; T, tetraploid germ cells; H, haploid germ cells.

tetraploid (4n) and haploid (n) germ cells were purified from rat testis by the technique of centrifugal elutriation, while testicular cells from 10-day-old rats served as a source of diploid germ cells. The isolated tetraploid and haploid germ cells, as checked by FACS analysis (Fig. 1A), were approximately 80 and 95% pure, respectively. The mRNA expression level in low-expressing cells, namely, the gametic diploid cells, was taken as a reference—except in the case of importin-8 and importin-11, where haploid cells were taken as the reference—to compare the difference (*n*-fold) in mRNA expression levels in other types of cells. Results of real-time PCR analysis of the expression pattern are shown in Fig. 1B. Importin-α1, importin-α3, importin-7, and importin-9 are expressed more or less at the same level in all the stages of germ cells (2n, 4n, and n). Importin-α2 is found to be expressed threefold higher in haploid cells and twofold higher in tetraploid cells compared to gametic diploid cells. Importin-β1 is expressed sevenfold higher in tetraploid cells and fivefold higher in haploid cells compared to gametic diploid cells. Importin-β2 is expressed threefold higher in tetraploid cells and twofold higher in haploid cells compared to gametic diploid cells. Importin-11 expression is fourfold higher in gametic diploid cells and sixfold higher in tetraploid cells compared to haploid cells. Importin-4 expression is 22-fold higher in tetraploid cells and 38-fold higher in haploid cells compared to gametic diploid cells. Importin-α4 is expressed 8-fold and 10-fold higher in tetraploid and haploid cells, respectively, which correlates with the previous report (20). Importin-α6 expression is 3-fold higher in tetraploid cells and 11-fold higher in haploid cells compared to gametic diploid cells. Importin-13 expression is 12-fold higher in tetraploid and haploid cells compared to gametic diploid cells. The importin-13 expression pattern is consistent with a previous report (51a), where importin-13 is shown to be involved in nuclear-cytoplasmic translocation of UBC9 during meiotic differentiation of mouse germ cells. Importin-β3 is expressed 12-fold higher in tetraploid cells and 27-fold higher in haploid cells compared to gametic diploid cells. Importin-8 is expressed fourfold higher in gametic diploid cells compared to tetraploid cells and haploid cells. Expression of NACA1 served as an internal control for normalization. We have also repeated the real-time PCR analysis of all the importin family members in biological replicate samples and found that the expression pattern is similar to the pattern shown in Fig. 1B (data not shown). Thus, in conclusion, we find that importin-β3 and importin-4 are the most highly expressed importin family members in haploid round spermatids. Recently, it has been shown that the relative importin concentration also determines the rate of import, and hence, the quantitative and qualitative difference in the expression pattern of each of the importins in a particular cell type might greatly influence the import of diverse nuclear proteins into the nucleus (52).

Physical interaction of TP2 with importin-4. From the results presented above, it is clear that expression of importins is differentially regulated during spermatogenesis and several importins are up-regulated in postmeiotic haploid cells. We surmised that one of the highly expressed importins in haploid round spermatids may have a role in the transport of TP2. To identify the importin involved in TP2 import, we initially carried out physical interaction studies with TP2 and importins using the immuno-pull-down assay. Recombinant TP2 was bound to anti-TP2-protein A-agarose beads and then incubated with recombinant importin-α1, importin-α3, importin-α4, importin-α6, importin-β1, importin-β2, importin-β3, importin-4, importin-7 and importin-9, and importin-13 (amino

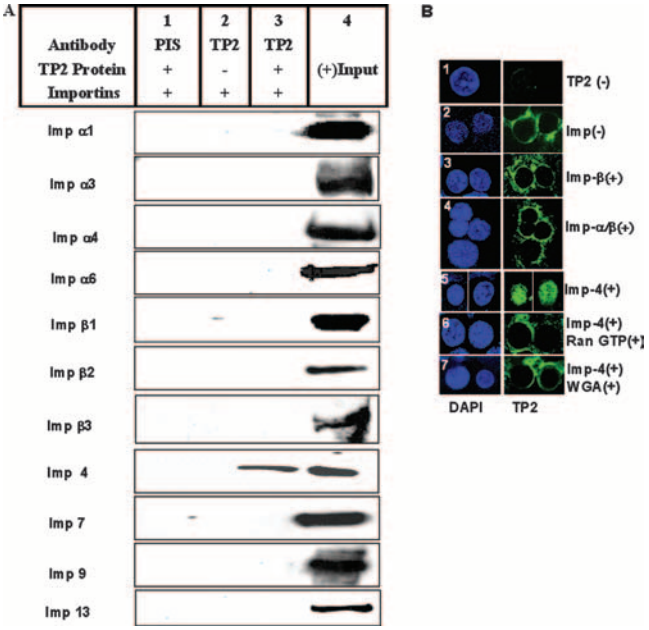

FIG. 2. Nuclear import of TP2 is mediated by importin-4. (A) Physical interaction of TP2 with different importins. TP2 (3 μg) was incubated with 3 μg of importin-α1, importin-α3, importin-α4, importin-α6, importin-β1, importin-β2, importin-β3, importin-4, importin-7, importin-9, and C-terminal importin-13 (amino acids 332 to 963) and then bound to protein A-agarose beads coupled with anti-TP2 antibodies. Preimmune sera (PIS) bound to protein A-agarose beads (lane 1) and TP2 antibody without TP2 protein (lane 2) were used as a negative control. The interacting proteins were analyzed by Western blot analysis using anti-GST antibodies for importin-α1 and importin-β1 and anti-His-tagged antibodies for other importins (Imp). (B) In vitro nuclear import assay. The import assay was carried out essentially using digitonin-permeabilized round spermatid cells (18). Recombinant importins like importin-α1, importin-β1, and importin-4 were used along with Ran and an energy regeneration system and recombinant TP2 as the cargo. After 30 min of incubation at 30°C, cells were fixed using 4% paraformaldehyde, and the localization of TP2 was monitored by indirect immunofluorescence using anti-TP2-monospecific antibodies and Alexa green-labeled anti-rabbit secondary antibodies. Panel 1, absence of TP2; panel 2, absence of importins; panel 3, presence of importin-β1 (1 μM); panel 4, presence of importin-α1/β1 heterodimer (1 μM each); panel 5, presence of importin-4 (1 μM); panel 6, importin-4 preincubated with RanGTP (5 μM); panel 7, digitonin-permeabilized round spermatids preincubated with WGA (0.4 mg/ml). DAPI, 4′,6′-diamidino-2-phenylindole.

acids 332 to 963). The bound proteins were separated by SDS-PAGE and probed with either anti-GST antibodies (for importin-α1, importin-α4, importin-13, importin-β3, and importin-β1 proteins) or anti-His-tag antibodies for the rest of the importins. The results presented in Fig. 2A clearly show that, among all the importin family members tested, only recombinant importin-4 physically interacted with TP2. In these experiments we have used mouse importin-β3 for our interaction studies with TP2. The mouse importin-β3 sequence shows 98.5% identity with the predicted amino acid sequence of rat importin-β3 (XM_224534). There are eight amino acid changes in the C-terminal region (harboring the cargo binding domain) and two changes in the N-terminal region. It remains to be seen whether rat importin-β3 can bind TP2 because of these minor amino acid changes present in its C-terminal domain.

Importin-4 mediates nuclear import of TP2. After demonstrating that importin-4 physically interacts with TP2, we carried out a series of experiments to see whether importin-4 mediates the transport of TP2 into the haploid spermatid nucleus. For this purpose, we reconstituted the import assay using various components of the energy-regenerating system and recombinant proteins in digitonin-permeabilized round spermatids (Fig. 2B). The localization of TP2 was monitored with monospecific TP2 antibodies. In the absence of any added importins, TP2 did not enter the spermatid nucleus (Fig 2B, panel 2). The addition of importin-β1 (Fig. 2B, panel 3) or importin-α1 and -β1 (panel 4) also did not facilitate the transport of TP2. When recombinant importin-4 was added to the transport assay mixture, most of the recombinant TP2 was observed inside the spermatid nucleus (Fig. 2B, panel 5). To further substantiate that this transport is physiologically relevant, we incubated recombinant RanGTP (which disrupts the interaction of importin and cargo) along with importin-4, in which case the import of TP2 was completely abolished (Fig. 2B, panel 6). Finally, we also observed that WGA also completely abolished the import of TP2 into the haploid spermatid nucleus (Fig. 2B, panel 7). WGA binds to nuclear pore complex protein, preventing their interaction with the importin receptors and thus blocking active transport (12).

All the above-described experiments were done with recombinant proteins and a reconstituted transport assay system. In order to demonstrate that importin-4 is present in the cytoplasm of round spermatids, which facilitates the transport of TP2, we carried out transport assays with digitonin-permeabilized round spermatids reconstituted with immunodepleted round spermatid cytosol as described in Materials and Methods. The specificity of anti-importin-4 polyclonal antibodies used in this experiment is evident from the Western blot analysis shown in Fig. 3A. The antibodies reacted with recombinant importin-4 and in vivo importin-4 but not any other importins in the round spermatid cytosol. The localization pattern of TP2 in this series of import assays is shown in Fig. 3C. The addition of control untreated round spermatid cytosol did facilitate the import of TP2 inside the haploid nucleus (Fig. 3C, panel 2), which is energy dependent (panel 3). On the other hand, when endogenous importin-4 was immunodepleted using anti-importin-4 antibodies, the round spermatid cells failed to facilitate the import of TP2 (Fig. 3C, panel 4). The addition of exogenous recombinant importin-4 to the immunodepleted cytosol restored the import of TP2 (Fig. 3C, panel 5). The Western blot analysis shown in Fig. 3B confirmed the complete absence of importin-4 in the immunodepleted cytosol. The Coomassie blue-stained pattern of cytosol before and after immunodepletion showed very similar protein profiles. Figure 3C (panels 6 and 7) shows that the import of TP2 was blocked by RanGTP as well as WGA, substantiating the conclusion that the import of TP2 follows the well-established pathway through the nuclear pore complex. Importin-4-depleted cytosol also failed to import VDR, which is a known cargo transported by importin-4 (38). In order to confirm that the importin-depleted cytosol is functionally active and can still support the transport of cargoes mediated by other importins, we tested the import of PTB using importin-4-depleted cytosol.

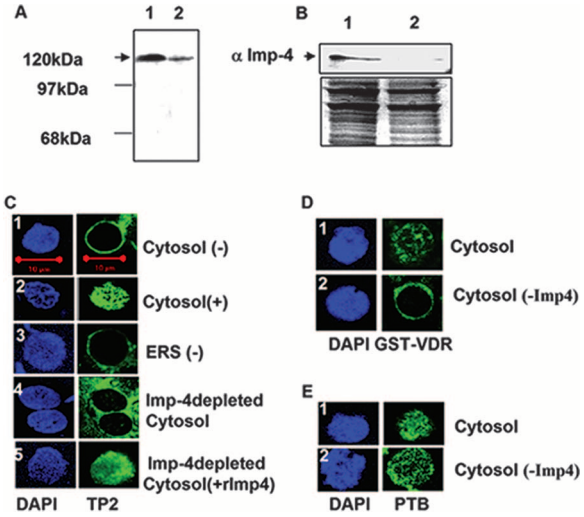

FIG. 3. In vitro nuclear import of TP2 with round spermatid cytosol. (A) Western blot analysis of round spermatid cytosol proteins with anti-importin-4 antibodies. Lane 1, recombinant importin-4; lane 2, round spermatid cytosol. (B) Western blot analysis of round spermatid cytosol with anti-importin-4 (α-Imp-4) antibodies before and after immunodepletion. Lane 1, undepleted cytosol; lane 2, depleted cytosol. The bottom panel shows the Coomassie-stained pattern of depleted and undepleted cytosol. (C) Import assay. Panel 1, absence of cytosol; panel 2, with cytosol; panel 3, presence of cytosol but without an ATP-regenerating system; panel 4, importin-4-immunodepleted cytosol; panel 5, immunodepleted cytosol replenished with exogenous recombinant importin-4 (rImp4) (0.1 mg/ml) (scale bar, 10 μm). (D) Import assay for the VDR using importin-4-depleted cytosol (panel 2) and mock-depleted cytosol (panel 1). Localization of VDR after the import assay was detected by anti-GST polyclonal antibodies. (E) Import assay with PTB using importin-4-depleted cytosol (panel 2) and mock-depleted cytosol (panel 1). Localization of PTB after the import assay was detected by anti-PTB rabbit polyclonal antibodies. DAPI, 4′,6′-diamidino-2-phenylindole.

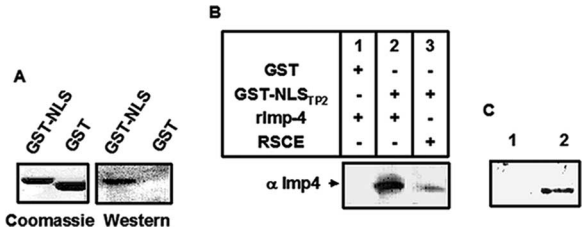

FIG. 4. Interaction of importin with NLS of TP2. (A) Western blot analysis of GST-NLS$_{TP2}$ fusion protein with anti-TP2 antibodies. The left panel shows the Coomassie blue-stained pattern, and the right panel shows Western blot analysis. (B) GST pull-down assay. Two micrograms of recombinant importin-4 (rImp-4) or cell extract was included with either GST or GST-NLS$_{TP2}$ prebound to glutathione-Sepharose. Interacting proteins were analyzed by Western blotting using antibodies against importin-4 (α Imp4). Lane 1, importin-4 pull-down with GST; lane 2, importin-4 pull-down with GST-NLS$_{TP2}$; lane 3, round spermatid extract (RSCE) pull-down by GST-NLS$_{TP2}$. (C) Effect of RanGTP on the interaction of importin-4 with GST-NLS$_{TP2}$. Lane 1, GST pull-down in the presence of RanGTP; lane 2, GST pull-down in the absence of RanGTP.

Results show that the import of PTB was not affected when we used importin-4-depleted cytosol; PTB is known to be imported by an importin-α/β-mediated pathway (45), thus unequivocally proving that importin-4 is involved in the transport of TP2.

NLS of TP2 (residues 87 to 95) interacts with importin-4. By various deletion analyses, we previously identified the NLS of TP2 to be localized to the region between amino acid residues 87 and 95, which is rich in basic amino acids (36). Since we have now identified importin-4 as being the receptor that carries the TP2 cargo into the nucleus, we were curious to examine whether the NLS of TP2 does physically interact with importin-4. We generated a GST fusion protein with the TP2$_{NLS}$ sequence at its C terminus. The recombinant GST-TP2$_{NLS}$ was authenticated by its reaction with anti-TP2 antibodies (Fig. 4A). The GST-TP2$_{NLS}$ fusion protein was immobilized on glutathione beads and used for subsequent pull-down experiments with either recombinant importin-4 or round spermatid cytosol. GST alone was used as a negative control for the nonspecific pull-down of proteins. The adsorbed proteins were separated by SDS-PAGE and probed with importin-4 antibodies after transferring them onto a nitrocellulose membrane. Results from the pull-down experiments are shown in Fig. 4B. It is clear that GST-TP2$_{NLS}$ interacts with recombinant importin-4 as well as endogenous importin-4 present in the round spermatid cytosol. GST alone did not bind to importin-4, showing the specificity of the interaction with TP2$_{NLS}$. Furthermore, the interaction of TP2$_{NLS}$ with importin-4 was abolished when RanGTP was added to the binding assay as shown in Fig. 4C. We also performed the GST-TP2$_{NLS}$ interaction study for all the six-His-tagged importins that we used for the immuno-pull-down experiment with TP2 (Fig. 2A). None of the other importins studied were found to interact with TP2$_{NLS}$, which shows the specificity of the interaction (data not shown).

Importin-4 mediates nuclear import of GST-fused TP2$_{NLS}$. After demonstrating that TP2$_{NLS}$ physically interacts with importin-4, we examined whether importin-4 can mediate the transport of the GST-TP2$_{NLS}$ fusion protein. These experiments were carried out with digitonin-permeabilized round spermatids as described above, and the immunolocalization patterns after staining with anti-GST antibodies are shown in Fig. 5A. In the presence of importin-β or importin-α/β, GST-TP2$_{NLS}$ was restricted to the cytoplasm (Fig. 5A, panels 1 and 2), while importin-4 facilitated the transport of GST-TP2$_{NLS}$ into the round spermatid nucleus (panel 3). The addition of RanGTP blocked this importin-4-mediated transport of GST-TP2$_{NLS}$ (Fig. 5A, panel 4). We also used round spermatid cytosol as the source of importin, and it is clear from Fig. 5B that GST-TP2$_{NLS}$ could be transported into the haploid spermatid nucleus in the presence of round spermatid cytosol (panel 1). However, we did not observe any import of GST-TP2$_{NLS}$ in the presence of cytosol that had been immunodepleted of importin-4 (Fig. 5A, panel 2). Furthermore, RanGTP abolished the import of GST-TP2$_{NLS}$ (panel 3).

Identification of the TP2$_{NLS}$ binding pocket in importin-4. Since several importins including importin-α/β and orphan members have been described to be involved in the recognition and transport of a variety of cargoes, it would be interesting to see their 3D structural features that dictate their interaction specificity. So far, only the structures of importin-α and -β have been solved by X-ray crystallography to date (5–8, 28, 33, 34). It is evident from the crystal structure that importin-β is a

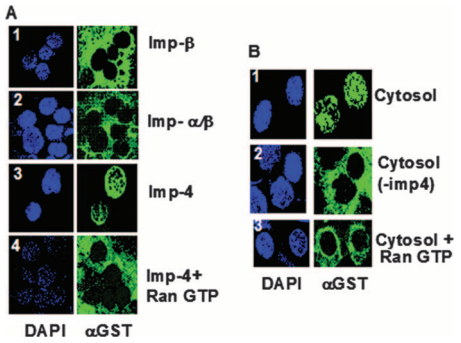

FIG. 5. Nuclear import of GST-NLS_{TP2} by importin-4. (A) In vitro nuclear import of GST-NLS_{TP2} using different recombinant importin proteins. Nuclear translocation of TP2 was reconstructed in digitonin-permeabilized round spermatids in the presence of importin-α/β (Imp-α/β), importin-β, or importin-4. Panel 1, presence of importin-β; panel 2, presence of importin-α/β heterodimer; panel 3, presence of importin-4; panel 4, importin-4 preincubated with RanGTP. Subcellular localization was probed with anti-GST antibodies (αGST), and the nucleus was stained with DAPI (4′,6′-diamidino-2-phenylindole). (B) In vitro nuclear import assay of GST-NLS_{TP2} using cytosol made from round spermatids as a source of importins (panel 1) and importin-4-immunodepleted cytosol (panel 2) and import assay in the presence of RanGTP (panel 3).

helicoidal molecule constructed from 19 HEAT repeats, each formed from a pair of alpha-helices connected by a short loop (3, 7). The N-terminal region of importin-β contains both a RanGTP binding domain and components of the nuclear pore complex binding domain, while the C-terminal region harbors the cargo-binding domain. In order to identify the $TP2_{NLS}$-interacting domain in importin-4, we have modeled the 3D structure of importin-4 using the importin-β1 structure (Fig. 6A) as the template. The final 3D model of importin-4 consisting of 900 amino acids from the N terminus, 36 alpha-helices, and 16 tandem HEAT repeats, which provides a superhelical conformation to its 3D structure (shown in Fig. 6B). A comparison of the tertiary structure revealed that the secondary structure elements of importin-4 are significantly similar to those of importin-β1 except that the importin-4 model possesses two antiparallel beta-sheets between helices 19 and 20, which are not found in the template structure (Fig. 6A and B). A superimposed image of importin-β1 and modeled importin-4 is shown in Fig. 6C. The amino acid sequence in importin-4, which is absent in importin-β1, contributes to the beta-sheet helix structure (Fig. 6D). The molecular docking studies showed that the $TP2_{NLS}$ has a single binding site between the 21st and 23rd helices (residues 529 to 609) (Fig. 6E). The surface view of the complex of the NLS and importin shows an NLS binding pocket (Fig. 6F). The NLS binding domain is acidic in nature, with a pI of 4.3. A similar molecular docking exercise with importin-α1 and importin-β1 did not reveal any interaction with $TP2_{NLS}$.

To further validate our modeling strategy, we performed a modeling and docking simulation study on the known structure of importin-β2 with its cargo, hnRNP A1-NLS (28), and importin-β1 with its cargo, the transcription factor SREBP2 (29). We observed through docking exercises that the NLS docked exactly between 8th and 20th HEAT repeats of importin-β2, coinciding with the position and orientation of docking as reported previously (28) (data not shown). A similar exercise also revealed a perfect match in the position and orientation of SREBP2-NLS with importin-β1 as reported previously (29) (data not shown).

To experimentally confirm that the region in importin-4 that we have identified by molecular docking studies does indeed interact with TP2, we performed in vitro pull-down experiments with the Δ529-609 deletion mutant of importin-4. There was no interaction of this deletion mutant with TP2, as can be seen from Fig. 7A, and the mutant also failed to facilitate the import of TP2 inside the nucleus (Fig. 7E). However, ΔC-terminal importin-4 could interact with TP2, which harbors the TP2-NLS-interacting domain (Fig. 7A). To rule out the possibility that the absence of an interaction with TP2 is due to the malfolding of the mutant importin-4 protein, we performed interaction studies of the wild-type protein and mutant importin-4 protein with TP2 and VDR, which is known to interact with importin-4 in its C-terminal region (amino acids 846 to 1081) (38). As can be seen in Fig. 7B, VDR was able to interact with both the wild type and the Δ529-609 deletion mutant of importin-4. However, there was no interaction of GST-VDR with ΔC-terminal importin-4, as it lacks a VDR-interacting domain (Fig. 7B). RanGTP is known to interact with importins in its N-terminal domain, as depicted in Fig. 6A. Interaction studies with wild-type and Δ529-609 importin-4 with its RanGTP showed that RanGTP interacts with wild-type as well as mutant importin-4 (Fig. 7D), indicating that the N-terminal domain is properly folded in this deletion mutant. Thus, all these experiments confirm that the stretch of amino acids from residues 529 to 609 of importin-4 is indeed involved in its interaction with TP2.

Nuclear import of TP1 is a passive process. TP1 (6.5 kDa) is another major basic nuclear protein comprising about 55% of chromatin proteins in elongating spermatids. To examine whether TP1 also utilizes a similar import pathway, we performed import assays using TP1 as cargo. The results presented in Fig. 7F (panels 1 and 2) show that the import of TP1 occurs in both the presence and absence of cytosol and also in the absence of energy regeneration systems (panel 3). Preincubation of digitonin-permeabilized round spermatid cells with WGA also had no effect on the nuclear import of TP1 (Fig. 7F, panel 4). Thus, TP1 is imported into the haploid spermatid nucleus by a passive process.

DISCUSSION

Import of nuclear proteins (of greater than 45 kDa) from the cytoplasm is a highly regulated process, and the key step is the recognition of the NLS signal by one of the importin/karyopherin family members. Importins can be classified into three groups, namely, α, β, and orphans. It is generally believed that several importins have evolved so as to recognize the NLSs of the nuclear protein cargoes, which are both definitive and fuzzy (7, 28, 29). We have been studying the various molecular aspects of chromatin remodeling that occur during mammalian spermiogenesis following meiotic division wherein there is a dramatic change in the chromatin structure during stages 12 to 19. The testis-specific proteins TP1 and TP2 are two major nuclear proteins that replace nearly 90% of the histones and their variants during this stage. The spermatids at this stage

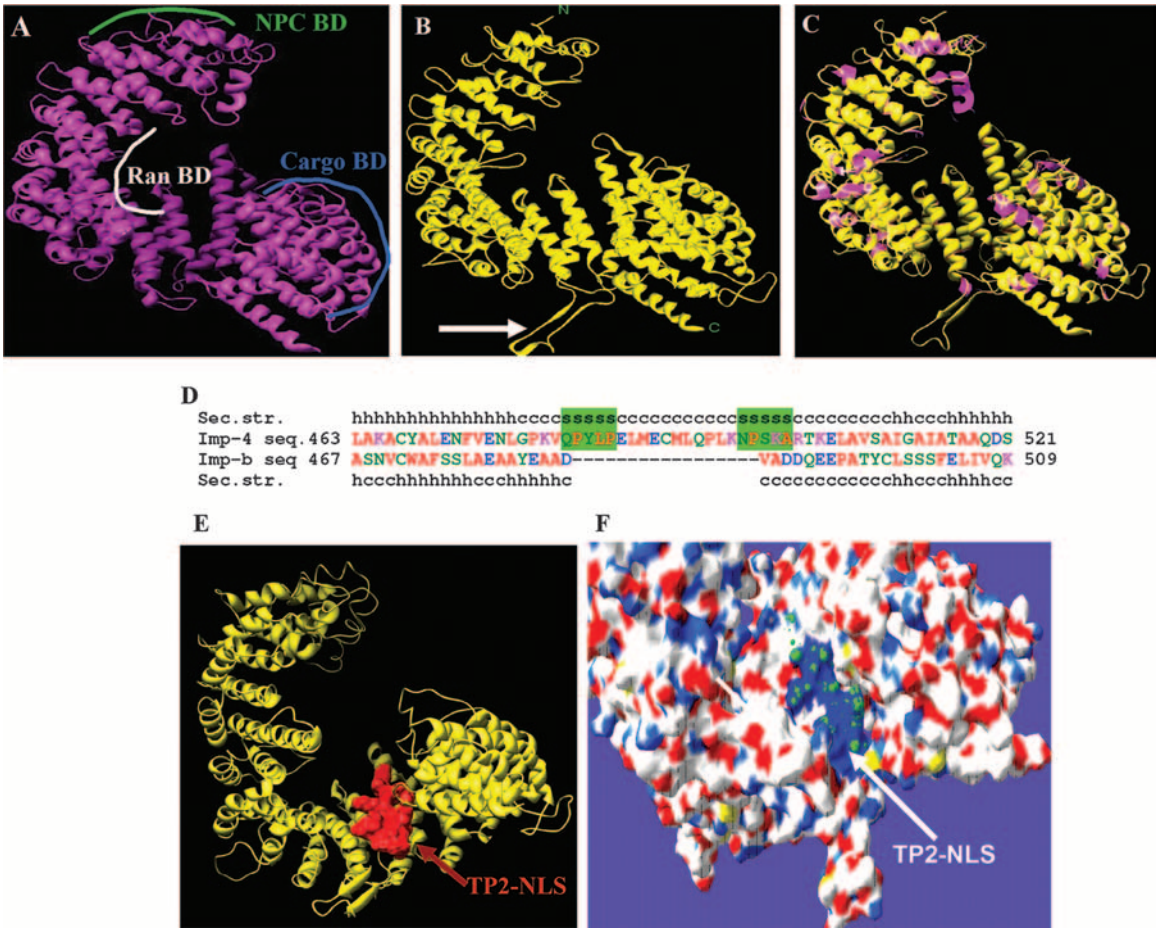

FIG. 6. Schematic representation of the 3D structure of the importin-4 model using importin-β1 as a template. (A) Ribbon diagram of human importin-β1. The N-terminal nuclear pore complex binding domain (NPC BD) (labeled in green), the RanGTP binding domain (labeled in white), and the C-terminal cargo binding domain (labeled in blue) are shown. (B) Ribbon diagram of the predicted structure of rat importin-4 protein in the same orientation. This superhelical structure is an alternate arrangement of 36 helices and loops. Two antiparallel beta-sheets that are not present in the importin-β1 structure are prominently seen in this structure (arrow). (C) Structural superimposition of importin-β (magenta) and importin-4 (yellow). The arrow indicates the antiparallel beta-sheets present in importin-4. (D) Representative amino acid sequence alignment showing amino acids (with shade) in importin-4 (Imp-4) contributing to the beta-sheet structure, which is absent in importin-β1 (h, helix; c, random coil; s, beta-sheet). (E) Importin-4 (yellow) docked with $TP2_{NLS}$ (red). The position of docking of $TP2_{NLS}$, shown by an arrow, lies in the region between helices 21 to 23 corresponding to the amino acid stretch at residues 529 to 609 of importin-4. (F) Surface view of the NLS binding pocket in importin-4. The surface view of the complex shows the pocket structure rich in acidic charge in which the NLS is embedded completely. Acidic and basic surfaces of the protein are shown in red and blue, respectively, and the arrow indicates the $TP2_{NLS}$ (blue) buried inside the NLS binding pocket.

have to cope with the import of these highly basic proteins. In this report, we have addressed the molecular components of the import machinery in the round spermatids that are involved in the import of TP1 and TP2.

From the results of our relative expression study of different importins in rat spermatogenic cells by real-time PCR (Fig. 1B) and expression studies of mouse importin-α and -β proteins by other groups (20, 31), it is clear that different importins have a distinct pattern of expression in testicular cells, which might have specific roles in the nuclear import of different cargoes during different stages of spermatogenesis. Of all the importin family members we have studied by real-time PCR analysis, we observed that importin-β3 and importin-4 are highly expressed in haploid spermatids compared to gametic diploid cells. We previously localized the NLS sequence of TP2 to ^{87}GKVSKRKAV^{95}, which defines its nuclear import that was dependent on cytosol and ATP (36, 51). The series of experiments described here involving both the physical interaction studies using an immuno-pull-down technique and in vitro transport assays have clearly demonstrated that it is importin-4 that is involved in the transport of TP2 into the haploid spermatid nucleus. Importin-4 belongs to the importin-β-related family (also called orphan importin) discovered only recently (25). The two protein cargoes that have been identified for importin-4 are VDR (38) and rpS3a (25), both of which are also basic proteins. Thus, TP2 becomes the third cargo to be imported by importin-4. Since all the three cargoes identified so far are basic in nature, it is quite likely that importin-4 might have specifically evolved to transport highly basic proteins.

Since importin-4 had the highest homology with importin-β1 and since its crystal structure has been determined, we mod-

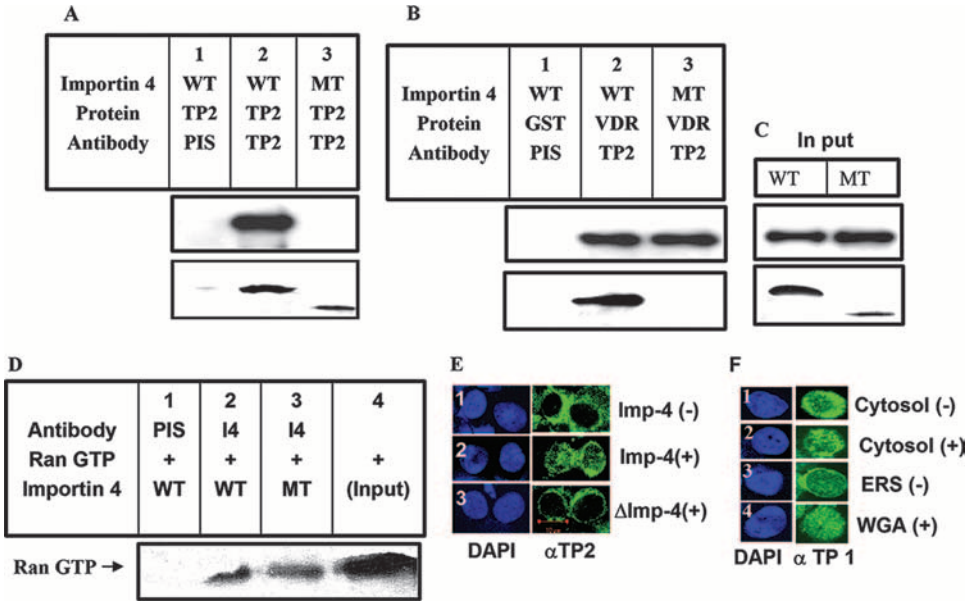

FIG. 7. Identification of $TP2_{NLS}$ binding pocket in importin-4. (A) Immuno-pull-down experiments with mutant importin-4 lacking amino acids 529 to 609 with TP2 (top) and mutant importin-4 lacking C-terminal amino acids 647 to 1081 (bottom) as described in the legend to Fig. 2A. Lane 1, preimmune sera (PIS) with wild-type (WT) importin-4 and TP2 protein; lane 2, TP2 antibody with wild-type importin-4 TP2 protein; lane 3, TP2 antibody with mutant (MT) importin-4 and TP2. (B) A GST-VDR pull-down experiment for mutant (Δ529–609) and wild-type importin-4 (top) and GST-VDR with wild-type importin-4 and ΔC-terminal importin-4 (bottom) was carried out as described in the legend to Fig. 4B. Lane 1, GST with wild-type importin-4; lane 2, GST-VDR with wild-type importin-4; lane 3, GST-VDR interaction with mutant importin-4. (C) Fifty percent input for both wild-type (lane 1) and mutant (lane 2) importin-4. (D) Immuno-pull-down of RanGTP with wild-type and Δ529–609 importin. RanGTP was detected with the His-tagged antibody. Lane 1, preimmune sera with wild-type importin-4 (I4); lane 2, immune serum with wild-type importin-4; lane 3, immune serum with Δ529–609 importin-4; lane 4, input RanGTP used for pull-down studies with importin-4. (E) Nuclear import of TP2 with Δimportin-4 (Δ529–609). The import assay was carried out as described in Materials and Methods. Panel 1, import assay in the absence of wild-type importin-4; panel 2, import assay in the presence of wild-type importin-4; panel 3, import assay in the presence of Δimportin-4 (scale bar, 10 μm). (F) Nuclear import of TP1. An in vitro import assay using TP1 as a cargo was carried out as described above for TP2. Panel 1, import assay in the presence of cytosol; panel 2, import assay in the absence of cytosol; panel 3, import assay in the absence of an energy regeneration system; panel 4, import assay in the presence of WGA. DAPI, 4′,6′-diamidino-2-phenylindole.

eled the 3D structure of importin-4. The overall structure of importin-4 is similar to that of importin-β1 except for an antiparallel beta-sheet between helices 19 and 20 (Fig. 6A, panels 1 and 2). Molecular docking studies have aided us in identifying the $TP2_{NLS}$ binding pocket within importin-4. Our modeling approach was also substantiated by similar modeling and docking simulation studies with the known structure of importin-β1 and importin-β2 and their cargoes, hnRNP A1 and SREBP2, respectively.

This theoretical prediction of the $TP2_{NLS}$ binding pocket was further confirmed experimentally using deletion mutants of importin-4 by in vitro interaction experiments as well as import assays. The interaction study with VDR and importin-4 has identified the C-terminal region of importin-4 as being the cargo interaction domain corresponding to amino acids 846 to 1081 (38). This is quite different from the region that we have identified for TP2 in the present study, which encompasses amino acids 529 to 609. Several control experiments with various deletion mutants of importin-4 and their interaction with TP2, VDR, and RanGTP clearly demonstrated that this region in importin-4 is the $TP2_{NLS}$-interacting domain.

The molecular mechanisms that underlie the recognition of the protein cargoes by their transport receptor or importins are rather poorly understood. The amino acid sequence differences among the members of the importin family of proteins might contribute to the diversity of the cargoes that they interact with to facilitate their import into the nucleus. Attempts are now being made to determine the crystal structure of importin complexed with its appropriate NLS to identify the cargo binding sites. To date, few such structures have been solved in importin-β proteins complexed with their cargoes. These structures are importin-β1 bound to the nonclassical NLS of PTHrP (6); importin-β bound to SREBP2, a transcription factor (29); and importin-β2 bound to hnRNP A1 (28). From these studies, it is becoming clear that the general features that govern this recognition process still seem to be elusive.

While all the evidence presented in this communication has shown that TP2 is imported into the nucleus through classical import pathways involving importin-4, the import of another major basic spermatid nuclear protein, TP1, was found to be achieved through a passive diffusion process. Both TP1 and TP2 are small basic proteins, and the fact that TP2 has taken the route of a specific receptor-mediated import mechanism suggests that its import into the nucleus needs to be a regulated event. During the final stages of spermiogenesis, TPs are further replaced by protamines p1 and p2. Since protamines are also highly basic and abundant proteins in mature spermatozoa, it remains to be seen whether they are imported by a

passive diffusion process, as in the case of TP1, or whether a specific transport receptor mechanism is involved.

ACKNOWLEDGMENTS

This work was financially supported from grants from the Department of Biotechnology, New Delhi, India. M. M. Pradeepa is supported by a fellowship from the Council of Scientific and Industrial Research, New Delhi, India. M. R. S. Rao thanks the Department of Science and Technology for the J. C. Bose fellowship.

We thank D. Gorlich, M. Kohler, Y. Yonida, and D. Forbes for plasmid constructs of importins and Noa Noy for the VDR cDNA clone. We thank V. Ramesh and T. C. Keerthi from our laboratory for PTB protein and testicular cDNAs, respectively. We thank B. S. Suma and G. N. Bharath for help in confocal microscopy and protein purification, respectively.

REFERENCES

1. **Adam, E. J., and S. A. Adam.** 1994. Identification of cytosolic factors required for nuclear location sequence-mediated binding to the nuclear envelope. J. Cell Biol. **125:**547–555.
2. **Adam, S. A., and L. Gerace.** 1991. Cytosolic proteins that specifically bind nuclear location signals are receptors for nuclear import. Cell **66:**837–847.
3. **Andrade, M. A., C. Petosa, S. I. O'Donoghue, C. W. Muller, and P. Bork.** 2001. Comparison of ARM and HEAT protein repeats. J. Mol. Biol. **309:** 1–18.
4. **Aratani, S., T. Oishi, H. Fujita, M. Nakazawa, R. Fujii, N. Imamoto, Y. Yoneda, A. Fukamizu, and T. Nakajima.** 2006. The nuclear import of RNA helicase A is mediated by importin-alpha3. Biochem. Biophys. Res. Commun. **340:**125–133.
5. **Chen, M. H., I. Ben-Efraim, G. Mitrousis, N. Walker-Kopp, P. J. Sims, and G. Cingolani.** 2005. Phospholipid scramblase 1 contains a nonclassical nuclear localization signal with unique binding site in importin alpha. J. Biol. Chem. **280:**10599–10606.
6. **Cingolani, G., J. Bednenko, M. T. Gillespie, and L. Gerace.** 2002. Molecular basis for the recognition of a nonclassical nuclear localization signal by importin beta. Mol. Cell **10:**1345–1353.
7. **Cingolani, G., C. Petosa, K. Weis, and C. W. Muller.** 1999. Structure of importin-beta bound to the IBB domain of importin-alpha. Nature **399:**221–229.
8. **Conti, E., M. Uy, L. Leighton, G. Blobel, and J. Kuriyan.** 1998. Crystallographic analysis of the recognition of a nuclear localization signal by the nuclear import factor karyopherin alpha. Cell **94:**193–204.
9. **Dean, K. A., O. von Ahsen, D. Görlich, and H. M. Fried.** 2001. Signal recognition particle protein 19 is imported into the nucleus by importin 8 (RanBP8) and transportin. J. Cell Sci. **114:**3479–3485.
10. **Fagerlund, R., L. Kinnunen, M. Köhler, I. Julkunen, and K. Melén.** 2005. NF-κB is transported into the nucleus by importin α3 and importin α4. J. Biol. Chem. **280:**15942–15951.
11. **Fassati, A., D. Gorlich, I. Harrison L. Zaytseva, and J. M. Mingot.** 2003. Nuclear import of HIV-1 intracellular reverse transcription complexes is mediated by importin 7. EMBO J. **22:**3675–3685.
12. **Finlay, D. R., D. D. Newmeyer, T. M. Price, and D. J. Forbes.** 1987. Inhibition of in vitro nuclear transport by a lectin that binds to nuclear pores. J. Cell Biol. **104:**189–200.
13. **Fried, H., and U. Kutay.** 2003. Nucleocytoplasmic transport: taking an inventory. Cell. Mol. Life Sci. **60:**1659–1688.
14. **Friedrich, B., C. Quensel, T. Sommer, E. Hartmann, and M. Köhler.** 2006. Nuclear localization signal and protein context both mediate importin specificity of nuclear import substrates. Mol. Cell. Biol. **26:**8697–8709.
15. **García-Blanco, M. A., S. F. Jamison, and P. A. Sharp.** 1989. Identification and purification of a 62,000-dalton protein that binds specifically to the polypyrimidine tract of introns. Genes Dev. **3:**1874–1886.
16. **Gorlich, D., S. Prehn, R. A. Laskey, and E. Hartmann.** 1994. Isolation of a protein that is essential for the first step of nuclear protein import. Cell **79:**767–778.
17. **Görlich, D., and U. Kutay.** 1999. Transport between the cell nucleus and the cytoplasm. Annu. Rev. Cell Dev. Biol. **15:**607–660.
18. **Gorlich, D., F. Vogel, A. D. Mills, E. Hartmann, and A. L. Ronald.** 1995. Distinct functions for the two importin subunits in nuclear protein import. Nature **377:**246–248.
19. **Henderson, B. R., and P. Percipalle.** 1997. Interactions between HIV Rev and nuclear import and export factors: the Rev nuclear localisation signal mediates specific binding to human importin-β. J. Mol. Biol. **274:**693–707.
20. **Hogarth, C. A., S. Calanni, D. A. Jans, and K. L. Loveland.** 2006. Importin alpha mRNAs have distinct expression profiles during spermatogenesis. Dev. Dyn. **235:**253–262.
21. **Imamoto, N., T. Shimamoto, T. Takao, T. Tachibana, S. Kose, M. Matsubae, T. Sekimoto, Y. Shimonishi, and Y. Yoneda.** 1995. In vivo evidence for involvement of a 58-kDa component of nuclear pore-targeting complex in nuclear protein import. EMBO J. **14:**3617–3626.
22. **Izaurralde, E., U. Kutay, C. von Kobbe, I. W. Mattaj, and D. Görlich.** 1997. The asymmetric distribution of the constituents of the Ran system is essential for transport into and out of the nucleus. EMBO J. **16:**6535–6547.
23. **Jäkel, S., W. Albig, U. Kutay, F. R. Bischoff, K. Schwamborn, D. Doenecke, and D. Görlich.** 1999. The importin beta/importin 7 heterodimer is a functional nuclear import receptor for histone H1. EMBO J. **18:**2411–2423.
24. **Jakel, S., and D. Gorlich.** 1998. Importin β, transportin, RanBP5 and RanBP7 mediate nuclear import of ribosomal proteins in mammalian cells. EMBO J. **17:**4491–4502.
25. **Jakel, S., J. M. Mingot, P. Schwarzmaier, E. Hartmann, and D. Gorlich.** 2002. Importins fulfil a dual function as nuclear import receptors and cytoplasmic chaperones for exposed basic domains. EMBO J. **21:**377–386.
26. **Jans, D. A., and S. Hubner.** 1996. Regulation of protein transport to the nucleus: central role of phosphorylation. Physiol. Rev. **76:**651–685.
27. **Kotera, I., T. Y. Sekimoto, Miyamoto, T. Saiwaki, E. H. Nagoshi, H. Sakagami, H. Kondo, and Y. Yoneda.** 2005. Importin alpha transports CaMKIV to the nucleus without utilizing importin beta. EMBO J. **24:**942–951.
28. **Lee, B. J., A. E. Cansizoglu, K. E. Suel, T. H. Louis, Z. Zhang, and Y. M. Chook.** 2006. Rules for nuclear localization sequence recognition by karyopherin beta 2. Cell **126:**543–558.
29. **Lee, S. J., T. Sekimoto, E. Yamashita, E. Nagoshi, A. Nakagawa, N. Imamoto, M. Yoshimura, H. Sakai, K. T. Chong, and T. Tsukihara.** 2003. The structure of importin-beta bound to SREBP-2: nuclear import of a transcription factor. Science **302:**1571–1575.
30. **Liu, L., K. M. McBride, and N. C. Reich.** 2005. STAT3 nuclear import is independent of tyrosine phosphorylation and mediated by importin-α3. Proc. Natl. Acad. Sci. USA **102:**8150–8155.
31. **Loveland, K. L., C. Hogarth, A. Szczepny, S. M. Prabhu, and D. A. Jans.** 2006. Expression of nuclear transport importins beta 1 and beta 3 is regulated during rodent spermatogenesis. Biol. Reprod. **74:**67–74.
32. **Maiyar A C., M. L. Leong, and G. L. Firestone.** 2003. Importin-alpha mediates the regulated nuclear targeting of serum- and glucocorticoid-inducible protein kinase (Sgk) by recognition of a nuclear localization signal in the kinase central domain. Mol. Biol. Cell **14:**1221–1239.
33. **Matsuura, Y., A. Lange, M. Harreman, A. Corbett, and M. Stewart.** 2003. Structural basis for Nup2p function in cargo release and karyopherin recycling in nuclear import. EMBO J. **22:**5358–5369.
34. **Matsuura, Y., and M. Stewart.** 2005. Nup50/Npap60 function in nuclear protein import complex disassembly and importin recycling. EMBO J. **24:** 3681–3689.
35. **McBride, K. M., G. Banninger, C. McDonald, and N. C. Reich.** 2002. Regulated nuclear import of the STAT1 transcription factor by direct binding of importin-α. EMBO J. **21:**1754–1763.
36. **Meetei, A. R., K. S. Ullas, and M. R. S. Rao.** 2000. Identification of two novel zinc finger modules and nuclear localization signal in rat spermatidal protein TP2 by site-directed mutagenesis. J. Biol. Chem. **275:**38500–38507.
37. **Mingot, J. M., S. Kostka, R. Kraft, E. Hartmann, and D. Gorlich.** 2001. Importin 13: a novel mediator of nuclear import and export. EMBO J. **20:**3685–3694.
38. **Miyauchi, Y., T. Michigami, N. Sakaguchi, T. Sekimoto, Y. Yoneda, J. W. Pike, M. Yamagata, and K. Ozono.** 2005. Importin 4 is responsible for ligand-independent nuclear translocation of vitamin D receptor. J. Biol. Chem. **280:**40901–40908.
39. **Moore, M. S., and G. Blobel.** 1994. Purification of a Ran-interacting protein that is required for protein import into the nucleus. Proc. Natl. Acad. Sci. USA **91:**10212–10216.
40. **Moore, J. D., J. Yang, R. Truant, and S. Kornbluth.** 1999. Nuclear import of Cdk/cyclin complexes: identification of distinct mechanisms for import of Cdk2/cyclin E and Cdc2/cyclin B1. J. Cell Biol. **144:**213–224.
41. **Moroianu, J., G. Blobel, and A. Radu.** 1995. Previously identified protein of uncertain function is karyopherin alpha and together with karyopherin beta docks import substrate at nuclear pore complexes. Proc. Natl. Acad. Sci. USA **92:**2008–2011.
42. **Plafker, S. M., and I. G. Macara.** 2000. Importin-11, a nuclear import receptor for the ubiquitin-conjugating enzyme, UbcM2. EMBO J. **19:**5502–5513.
43. **Plafker, S. M., and I. G. Macara.** 2002. Ribosomal protein L12 uses a distinct nuclear import pathway mediated by importin 11. Mol. Cell. Biol. **22:**1266–1275.
44. **Pollard, V. W., W. M. Michael, S. Nakielny, M. C. Siomi, F. Wang, and G. Dreyfuss.** 1996. A novel receptor-mediated nuclear protein import pathway. Cell **86:**985–994.
45. **Romanelli, M. G., and C. Morandi.** 2002. Importin alpha binds to an unusual bipartite nuclear localization signal in the heterogeneous ribonucleoprotein type I. Eur. J. Biochem. **269:**2727–2734.
46. **Sudhakar, L., and M. R. S. Rao.** 1990. Stage-dependent changes in localization of a germ cell-specific lamin during mammalian spermatogenesis. J. Biol. Chem. **265:**22526–22532.
47. **Takizawa, C. G., K. Weis, and D. O. Morgan.** 1999. Ran-independent nu-

clear import of cyclin B1-Cdc2 by importin beta. Proc. Natl. Acad. Sci. USA **96:**7938–7943.

48. **Tao, T., J. Lan, G. L. Lukacs, R. J. Haché, and F. Kaplan.** 2006. Importin 13 regulates nuclear import of the glucocorticoid receptor in airway epithelial cells. Am. J. Respir. Cell Mol. Biol. **35:**668–680.
49. **Truant, R., and B. R. Cullen.** 1999. The arginine-rich domains present in human immunodeficiency virus type 1 Tat and Rev function as direct importin β-dependent nuclear localization signals. Mol. Cell. Biol. **19:**1210–1217.
50. **Tseng, S. F., C. Y. Chang, K. J. Wu, and S. C. Teng.** 2005. Importin KPNA2 is required for proper nuclear localization and multiple functions of NBS1. J. Biol. Chem. **280:**39594–39600.
51. **Ullas, K. S., and M. R. S. Rao.** 2003. Phosphorylation of rat spermatidal protein TP2 by sperm-specific protein kinase A and modulation of its transport into the haploid nucleus. J. Biol. Chem. **278:**52673–52680.

51a. **Yamaguchi, Y. L., S. S. Tanaka, K. Yasuda, Y. Matsui, and P. P. L. Tam.** 2006. Stage-specific importin 13 activity influences meiosis of germ cells in the mouse. Dev. Biol. **297:**350–360.

52. **Yang, W., and M. S. Musser.** 2006. Nuclear import time and transport efficiency depend on importin beta concentration. J. Cell Biol. **174:**951–961.
53. **Zhao, M., C. R. Shirley, S. Mounsey, and M. L. Meistrich.** 2004. Nucleoprotein transitions during spermiogenesis in mice with transition nuclear protein Tnp1 and Tnp2 mutations. Biol. Reprod. **71:**1016–1025.